Geometric Multicut

Mikkel Abrahamsen* Panos Giannopoulos[†] Maarten Löffler[‡] Günter Rote[§]

March 17, 2022

Abstract

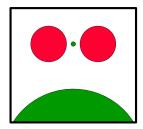
We study the following separation problem: Given a collection of colored objects in the plane, compute a shortest "fence" F, i.e., a union of curves of minimum total length, that separates every two objects of different colors. Two objects are separated if F contains a simple closed curve that has one object in the interior and the other in the exterior. We refer to the problem as GEOMETRIC k-CUT, where k is the number of different colors, as it can be seen as a geometric analogue to the well-studied multicut problem on graphs. We first give an $O(n^4 \log^3 n)$ -time algorithm that computes an optimal fence for the case where the input consists of polygons of two colors and n corners in total. We then show that the problem is NP-hard for the case of three colors. Finally, we give a (2-4/3k)-approximation algorithm.

^{*}Basic Algorithms Research Copenhagen (BARC), University of Copenhagen, Universitetsparken 1, DK-2100 Copenhagen \emptyset , Denmark. miab@di.ku.dk. Supported by the Innovation Fund Denmark through the DABAI project. BARC is supported by the VILLUM Foundation grant 16582.

[†]giCenter, Department of Computer Science, City University of London, EC1V 0HB, London, United Kingdom. panos.giannopoulos@city.ac.uk.

[‡]Department of Information and Computing Sciences, Utrecht University, The Netherlands. m.loffler@uu.nl. Partially supported by the Netherlands Organisation for Scientific Research (NWO); 614.001.504.

[§]Institut für Informatik, Freie Universität Berlin, Takustrae 9, 14195 Berlin, Germany. rote@inf.fu-berlin.de.



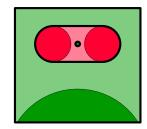


Figure 1: An instance with k=2 sets, red and green, with two disks each; the big green disk is only partially shown. The optimal cover has a hippodrome-shaped red set, with the small green disk as a hole, and an unbounded green set. The fence F has two components: the boundary of the hippodrome and the boundary of the small green disk.

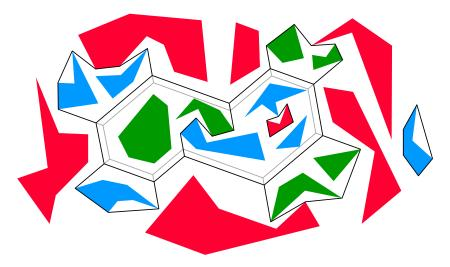


Figure 2: An instance of GEOMETRIC 3-CUT and an optimal fence in black. The fence contains a cycle that does not touch any object. The grey fence shows how the cycle can be shrunk without changing the total length of the fence (Lemma 2).

1 Introduction

Problem Definition. We are given k pairwise interior-disjoint, not necessarily connected, sets B_1, B_2, \ldots, B_k in the plane. We want to find a covering of the plane $\mathbb{R}^2 = \bar{B}_1 \cup \bar{B}_2 \cup \cdots \cup \bar{B}_k$ such that the sets \bar{B}_i are closed and interior-disjoint, $B_i \subseteq \bar{B}_i$ and the total length of the boundary $F = \bigcup_{i=1}^k \partial \bar{B}_i$ between the different sets \bar{B}_i is minimized.

We think of the k sets B_i as having k different colors and each set B_i as a union of simple geometric objects like circular disks and simple polygons. Examples are shown in Figure 1 and Figure 2. We call \bar{B}_i the territory of color i. The "fence" F is the set of points that separates the territories. (Alternatively, F is the set of points belonging to more than one territory.) As we can see, a territory can have more than one connected component.

An alternative view of the problem concentrates on the *fence*: A fence is defined as a union of curves F such that each connected component of $\mathbb{R}^2 \setminus F$ intersects at most one set B_i . An interior-disjoint covering as defined above gives, by definition, such a fence. Likewise, a fence F induces such a covering, by assigning each connected component of $\mathbb{R}^2 \setminus F$ to an appropriate territory \bar{B}_i . The total length of a fence F is also called the *cost* of F and is denoted as |F|.

In our paper, we will focus on the case where the input consists of simple polygons (with disjoint interiors) where the corners have rational coordinates. We denote this problem as $GEOMETRIC\ k\text{-}CUT$, Each input polygon is called an *object*. We use n to denote the total number of corners of the input polygons. We count the corners with multiplicity so that if a point is a corner of more objects, it is counted for each object individually.

The results can be extended to more general shapes as long as they are reasonably well behaved.

Even in this simple setting, the problem poses both geometric and combinatorial difficulties. A set B_i can consist of disconnected pieces, and the combinatorial challenge is to choose which of the pieces should be grouped into the same component of \bar{B}_i . The geometric task is to construct a network of curves that surrounds the given groups of objects and thus separates the groups from each other. For k=2 colors, optimal fences consist of geodesic curves around obstacles, which are well understood. As soon as the number k of colors exceeds 2, the geometry becomes more complicated, and the problem acquires traits of the geometric Steiner tree problem, as shown by the example in Figure 2.

The problem of enclosing a set of objects by a shortest system of fences has been considered with a single set B_1 by Abrahamsen et al. [1]. The task is to "enclose" the components of B_1 by a shortest system of fences. This can be formulated as a special case of our problem with k = 2 colors: We add an additional set B_2 , far away from B_1 and large enough so that it is never optimal to enclose B_2 . Thus, we have to enclose all components of B_1 and separate them from the unbounded region. In this setting, there will be no nested fences. Abrahamsen et al. gave an algorithm with running time O(n polylog n) for the case where the input consists of n unit disks.

Our Results. In Section 3, we show how to solve the case with k = 2 colors in time $O(n^4 \log^3 n)$. The algorithm works by reducing the problem to the multiple-source multiple-sink maximum flow problem in a planar graph. In Section 4, we show that already the case with k = 3 colors is NP-hard by a reduction from PLANAR POSITIVE 1-IN-3-SAT.

In Section 5, we discuss approximation algorithms. We first compare the optimal fence $F_{\mathcal{A}}$ consisting of line segments between corners of input polygons to the unrestricted optimal fence F^* . We show that $|F_{\mathcal{A}}| \leq 4/3 \cdot |F^*|$. After applying a (3/2 - 1/k)-approximation algorithm for the k-terminal multiway cut problem [4], we obtain a polynomial-time $(2 - \frac{4}{3k})$ -approximation algorithm for GEOMETRIC k-CUT (Theorem 16).

2 Structure of Optimal Fences

Lemma 1. An optimal fence F^* is a union of (not necessarily disjoint) closed curves, disjoint from the interior of the objects. Furthermore, F^* is the union of straight line segments of positive length. Consider two non-collinear line segments $\ell_1, \ell_2 \subset F^*$ with a common endpoint p. If p is not a corner of an object, then exactly three line segments meet at p and form angles of $2\pi/3$.

Proof. We first prove that the curves in F^* are disjoint from the interior of each object. To this end, consider any fence F in which some open curve $\pi \subset F$ is contained in the interior of an object $O \subset B_i$. Then the domains on both sides of π must be part of the territory \overline{B}_i . Hence, π can be removed from F while the fence remains feasible. That operation reduces the length, so F is not optimal.

We next show that F^* is the union of a set of closed curves. Suppose not. Let $F' \subset F^*$ be the union of all closed curves contained in F^* and let π be a connected component in $F^* \setminus F'$. Then π is the (not necessarily disjoint) union of a set of open curves, which do not contribute to the separation of any objects. Hence, $F^* \setminus \pi$ is a fence of smaller length than F^* , so F^* is not optimal.

In a similar way, one can consider the union L of all line segments of positive length contained in F^* , and if $F^* \setminus L$ is non-empty, a standard argument shows that a curve π in $F^* \setminus L$ can be replaced by line segments, thus reducing the total length.

The last claimed property is shared with the Euclidean Steiner minimal tree on a set of points in the plane, and it can be proved in the same way, see for example Gilbert and Pollak [9]: Suppose that the fence F contains two non-collinear line segments ℓ_1 and ℓ_2 sharing an endpoint p that is not a corner of an object. If the angle between ℓ_1 and ℓ_2 at p is less than $2\pi/3$, then parts of ℓ_1 and ℓ_2 can be replaced by three shorter segments. Hence, the angle between segments meeting at p is at least $2\pi/3$, and there can be at most three such line segments. If there are only two, one can make a shortcut. Therefore, there are exactly three segments, and they form angles of $2\pi/3$.

As it can be seen in Figure 2, optimal fences may contain cycles that do not touch any object. By the following lemma, such cycles can be eliminated without increasing the length. This will turn out to be useful in our design of approximation algorithms.

Lemma 2. Let N be the set of corners of the objects in an instance of GEOMETRIC k-CUT. There exists an optimal fence F^* with the property that $F^* \setminus N$ contains no cycles.

Proof. Let us look at a connected component T of $F^* \setminus N$. By Lemma 1, its leaves are in N. All other vertices have degree 3, and the incident edges meet at angles of $2\pi/3$. If T contains a cycle C, we can push the edges of C in a parallel fashion (forming an offset curve), as shown in Figure 2. This operation does not change the total length of T. This can be seen by looking at each degree-3 vertex v individually: We enclose v in a small equilateral triangle whose sides cut the edges at right angles, see Figure 3. It is an easy geometric fact that the sum of the distances from a point inside an equilateral triangle to the three sides is constant. This implies that the length of the fence inside the triangle is unchanged by the offset operation. The portions of C outside the triangles are just translated and do not change their lengths either.

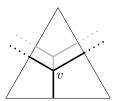


Figure 3: Offsetting the cycle does not change the total length of the fence inside the triangle.

As we offset the cycle C, an edge of C must eventually hit a corner of an object. Another conceivable possibility is that an edge of C between two degree-3 vertices is reduced to a point, but this can be excluded because it would lead to an optimal fence violating Lemma 1.

In this way, the cycles of T can be eliminated one by one.

3 The Bicolored Case

In this section we consider the case of k=2 different colors. Let N be the set of all corners of the objects. A line segment is said to be *free* if it is disjoint from the interior of every object. A vertex v of an optimal fence cannot have degree 3 or more unless $v \in N$, as otherwise two of the regions meeting at v would be part of the same territory and could be merged, thus reducing the length. We therefore get the following consequence of Lemma 1.

Lemma 3. An optimal fence consists of free line segments with endpoints in N.

Let S be the set of all free segments with endpoints in N. S includes all edges of the objects. Let \mathcal{A} be the arrangement induced by S, see Figure 4. Consider an optimal fence F^* and the associated territories \bar{B}_1 and \bar{B}_2 . Lemma 3 implies that F^* is contained in \mathcal{A} . Thus, each cell of \mathcal{A} belongs entirely either to \bar{B}_1 or \bar{B}_2 . The objects are cells of \mathcal{A} whose classification (i.e., membership of \bar{B}_1 versus \bar{B}_2)

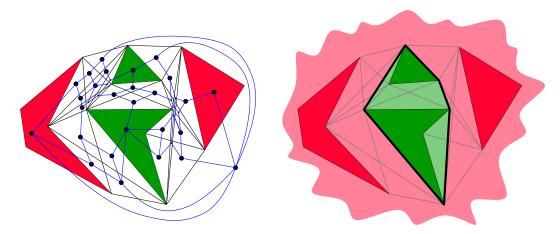


Figure 4: Left: The arrangement \mathcal{A} induced by an instance of GEOMETRIC 2-CUT with two green and two red objects. The edges of the dual graph G are blue. Right: The optimal solution.

is fixed. In order to find F^* , we need to select the territory that each of the other cells belongs to. Since $|S| = O(n^2)$, \mathcal{A} has size $O(|S|^2) = O(n^4)$ and can be computed in $O(|\mathcal{A}|) = O(n^4)$ time [5]. For simplicity, we stick with the worst-case bounds. In practice, set S can be pruned by observing that the edges of an optimal fence must be *bitangents* that touch the objects in a certain way, because the curves of the fence are locally shortest.

Finding an optimal fence amounts to minimizing the boundary between \bar{B}_1 and \bar{B}_2 . This can be formulated as a minimum-cut problem in the dual graph G(V,E) of the arrangement \mathcal{A} . There is a node in V for each cell and a weighted edge in E for each pair of adjacent cells: the weight of the edge is the length of the cells' common boundary. Let $S_1, S_2 \subset V$ be the sets of cells that contain the objects of B_1, B_2 , respectively. We need to find the minimum cut that separates S_1 from S_2 . This can be obtained by finding the maximum flow in G from the sources S_1 to the sinks S_2 , where the capacities are the weights. As G is a planar graph, we can use the algorithm by Borradaile et al. [3] with running time $O(|V|\log^3|V|)$. The running time has since then been improved to $O(\frac{|V|\log^3|V|}{\log^2\log|V|})$ [8]. As $|V| = O(|S|^2) = O(n^4)$, we obtain the following theorem.

Theorem 4. GEOMETRIC 2-CUT can be solved in time
$$O(\frac{n^4 \log^3 n}{\log^2 \log n})$$
.

A similar algorithm has been described before in a slightly different context: image segmentation [10], see also [3]. Here, we have a rectangular grid of pixels, each having a given gray-scale value. Some pixels are known to be either black or white. The remaining pixels have to be assigned either the black or the white color. Each pixel has edges to its (at most four) neighbors. The weights of these edges can be chosen in such a way that the minimum cut problem corresponds to minimizing a cost function consisting of two parts: One part, the *data component*, has a term for each pixel, and it measures the discrepancy between the gray-value of the pixel and the assigned value. The other part, the *smoothing component*, penalizes neighboring pixels with similar gray-values that are assigned different colors.

4 Hardness of the Tricolored Case

We show how to construct an instance I of GEOMETRIC 3-CUT from an instance Φ of PLANAR POSITIVE 1-IN-3-SAT. For ease of presentation, we first describe the reduction geometrically, allowing irrational coordinates. We prove that if Φ is satisfiable, then I has a fence of cost M^* , whereas if Φ is not satisfiable, then the cost is at least $M^* + 1/50$. We then argue that the corners can be slightly moved to make a new instance I' with rational coordinates while still being able to distinguish whether Φ is satisfiable or not, based on the cost of an optimal fence.

In order to make the proof as simple as possible, we introduce a new specialized problem COLORED TRIGRID POSITIVE 1-IN-3-SAT in the following.

4.1 Auxiliary NP-complete problems

Definition 5. In the POSITIVE 1-IN-3-SAT problem, we are given a collection Φ of clauses containing exactly three distinct variables (none of which are negated). The problem is to decide whether there exists an assignment of truth values to the variables of Φ such that exactly one variable in each clause is true.

Definition 6. In the TRIGRID POSITIVE 1-IN-3-SAT problem, we are given an instance Φ of POSITIVE 1-IN-3-SAT together with a planar embedding of an associated graph $G(\Phi)$ with the following properties:

- $G(\Phi)$ is a subgraph of a regular triangular grid,
- for each variable x, there is a simple cycle v_x ,
- for each clause $C = \{x, y, z\}$, there is a path c_C and three vertical paths $\ell_x^C, \ell_y^C, \ell_z^C$ with one endpoint at a vertex of c_C and one at a vertex of each of v_x, v_y, v_z ,
- except for the described incidences, no edges share a vertex,
- all vertices have degree 2 or 3,

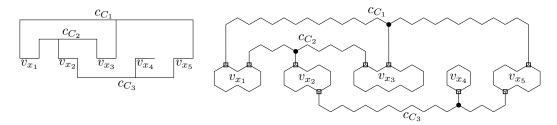


Figure 5: Left: An instance of PLANAR POSITIVE 1-IN-3-SAT for the formula $\Phi = C_1 \wedge C_2 \wedge C_3$ for $C_1 = x_1 \vee x_3 \vee x_5$, $C_2 = x_1 \vee x_2 \vee x_3$, and $C_3 = x_2 \vee x_4 \vee x_5$. Right: A corresponding instance of TRIGRID POSITIVE 1-IN-3-SAT. Clause vertices are drawn as dots and branch vertices as boxes.

- any two adjacent edges form an angle of π or $2\pi/3$,
- the number of vertices is bounded by a quadratic function of the size of Φ .

The problem is to decide whether Φ has a satisfying assignment.

Mulzer and Rote [13] showed that another problem, PLANAR POSITIVE 1-IN-3-SAT, is NP-complete, which is similar but uses a slightly different embedding with axis-parallel segments. It trivially follows that TRIGRID POSITIVE 1-IN-3-SAT is also NP-complete, see Figure 5.

Consider an instance $(\Phi, G(\Phi))$ of TRIGRID POSITIVE 1-IN-3-SAT. There are some vertices of degree three on the cycles v_x corresponding to each variable x in Φ , and these we denote as branch vertices of $G(\Phi)$. There is also one vertex of degree three on the path c_C corresponding to each clause C in Φ , which we denote as a clause vertex. Except for branch and clause vertices, at most two edges meet at each vertex.

Let \mathcal{C} be the set of all clause vertices (considered as geometric points). Removing \mathcal{C} from $G(\Phi)$ (considered as a subset of \mathbb{R}^2) splits $G(\Phi)$ into one connected component E_x for each variable x of Φ . The idea of our reduction to GEOMETRIC 3-CUT is to build a *channel* on top of E_x for each variable x. The channel has constant width 1/2 and contains E_x in the center. The channel contains small *inner* objects and is bounded by larger *outer objects* of another color. There will be two equally good ways to separate the inner and outer objects, namely taking an individual fence around each inner object and taking long fences along the boundaries of the channel that enclose as many inner objects as possible. Any other way of separating the inner from the outer objects will require more fence. These two optimal fences play the roles of x being true and false, respectively.

At the clause vertices where three regions E_x, E_y, E_z meet, we make a clause gadget that connect the three channels corresponding to x, y, z. The objects in the clause gadget can be separated using the least amount of fence if and only if one of the channels is in the state corresponding to true and the other two are in the false state. Therefore, this corresponds to the clause in Φ being satisfied.

In order to make this idea work, we first assign every edge of $G(\Phi)$ an *inner* and an *outer* color among {red, green, blue}. These will be used as the colors of the inner and outer objects of the channel later on. We require the following of the coloring:

- 1. The inner and outer colors of any edge are distinct.
- 2. Any two adjacent collinear edges have the same inner or outer color.
- 3. Any two adjacent edges that meet at an angle of $2\pi/3$ at a non-clause vertex have the same inner and the same outer color.
- 4. The inner colors of the three edges meeting at a clause vertex are red, green, blue in clockwise order, while the outer colors of the same edges are blue, red, green, respectively.

We now introduce the problem COLORED TRIGRID POSITIVE 1-IN-3-SAT, which we will reduce to GEOMETRIC 3-CUT.

Definition 7. In the COLORED TRIGRID POSITIVE 1-IN-3-SAT problem, we are given an instance $(\Phi, G(\Phi))$ of TRIGRID POSITIVE 1-IN-3-SAT together with a coloring of the edges of $G(\Phi)$ satisfying the above requirements. We want to decide whether Φ has a satisfying assignment.

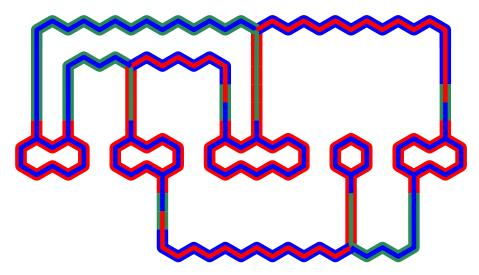


Figure 6: An instance of COLORED TRIGRID POSITIVE 1-IN-3-SAT based on the instance from Figure 5.

Lemma 8. The problem COLORED TRIGRID POSITIVE 1-IN-3-SAT is NP-complete.

Proof. Membership in NP is obvious. For NP-hardness, we reduce from TRIGRID POSITIVE 1-IN-3-SAT. Let $(\Phi, G(\Phi))$ be an instance of the latter and $G'(\Phi)$ be the graph obtained from $G(\Phi)$ by expanding the vertical paths ℓ_x^C , so that they have length at least 4. The cycles v_x and paths c_C are shifted up or down accordingly, see Figure 6. We specify the coloring of $G'(\Phi)$ below.

We color each triple of edges meeting at a clause vertex so that requirement 4 is met. In each of the paths c_C , we have colored one edge on each side of the clause vertex, and we use the colors of that edge to color the rest of the edges on that side. Next, we choose two distinct colors that we use as the inner and outer colors of all the cycles v_x containing the branch vertices. For each vertical path ℓ_x^C , the edge adjacent to the cycle v_x has to be colored with the same two colors.

It remains to color some edges of each vertical path ℓ_x^C . Since the vertical paths have length at least 4 and only the first and last edges have been colored, it is possible to change inner and outer color three times along each of them. The maximum number of changes is needed when the edge adjacent to a clause vertex has the inner and outer colors swapped as compared to the edge adjacent to a branch vertex, in which case exactly three changes are needed. Therefore, it is possible to adjust the colors so that the entire path gets colored. We have hence constructed an instance of COLORED TRIGRID POSITIVE 1-IN-3-SAT based on the same instance Φ of POSITIVE 1-IN-3-SAT that we were given.

4.2 Building a GEOMETRIC 3-SAT instance from tiles

Consider an instance $(\Phi, G(\Phi))$ of COLORED TRIGRID POSITIVE 1-IN-3-SAT that we will reduce to GEOMETRIC 3-CUT. We make the construction using hexagonal *tiles* of six different types, namely *straight*, *inner color change*, *outer color change*, *bend*, *branch*, and *clause* tiles. Each tile is a regular hexagon with side length $1/\sqrt{3}$ and hence has width 1. The tiles are rotated such that they have two horizontal edges.

The tiles are placed so that each tile is centered at a vertex p of $G(\Phi)$. Let G_p be the part of $G(\Phi)$ within distance 1/2 from p (recall that each edge of $G(\Phi)$ has length 1). Figure 7 shows the tiles and how they are placed according to the shape and colors of G_p .

In order to define the outer objects of a tile, we consider the straight skeleton offset [2] of G_p at distance 1/4. With the exception of the bend tile, this offset is the same as the Euclidean offset. By the outer and inner region, we mean the region of the tile outside, resp. inside, this offset. The outer objects cover the outer region, and every point is colored with the outer color of a closest edge in G_p . The inner region is empty except for the inner objects described in each case below. We suppose that p = (0,0).

The straight tile. If two collinear edges meet at p with the same inner and outer color, we use a straight tile. Suppose in this and the following two cases that G_p is the vertical line segment from

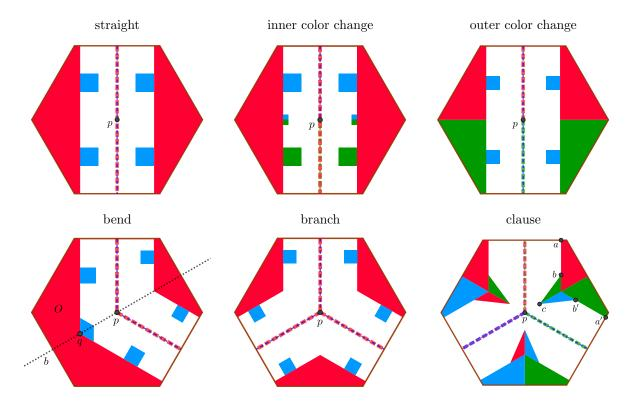


Figure 7: Different kinds of tiles used in the reduction to GEOMETRIC 3-CUT. The dashed colored segments show G_p and the inner and outer color of G_p . The tiles are colored accordingly. The points in the clause tile are defined so that ||ab|| = ||a'b'|| = 6/25 = 0.24 and ||bc|| = ||b'c|| = 1/4 = 0.25. Point c has coordinates $(x, x/\sqrt{3})$, where $x = \frac{13\sqrt{3}}{200} + 3/16 - \frac{\sqrt{-459+3900\sqrt{3}}}{400}$ is a solution to $10000x^2 + (-1300\sqrt{3} - 3750)x + 507 = 0$. The remaining points in the tile are given by rotations by angles $2\pi/3$ and $4\pi/3$ around p.

(0,-1/2) to (0,1/2)—tiles for edges of other slopes are obtained by rotation of the ones described here. There are four axis-parallel squares of the inner color of G_p with side length 1/8 centered at $(\pm(1/4-1/16),\pm1/4)$. This size is chosen so their total perimeter is 2, which is the length of the common boundary of the inner and outer regions.

The inner color change tile. If two collinear edges meet at p with different inner colors, we use an inner color change tile. There are again four squares colored in the inner color of the closest point in G_p . There are also four smaller axis-parallel squares with side length 1/28 centered at $(\pm(1/4-1/56), \pm 1/56)$, likewise colored in the inner color of the closest point in G_p . The size of these small squares is chosen so that they can be individually enclosed using fences of total length $14 \cdot 1/28 = 1/2$, which is the width of the inner region.

The outer color change tile. If two collinear edges meet at p with different outer colors, we use an outer color change tile. There are four axis-parallel squares of the inner color of G_p with side length 3/32. Their centers are $(\pm(1/4-3/64),\pm1/4)$. The size of these squares is chosen so that their total perimeter is 2-1/2=3/2.

The bend tile. If two non-collinear edges meet at p, we use a bend tile. Consider the case where G_p is the vertical line segment from p to (0,1/2) and the segment of length 1/2 from p with direction $(\cos \pi/6, -\sin \pi/6)$. The other cases are obtained by a suitable rotation of this tile. There is an axis parallel square of side length $x = \frac{6+\sqrt{3}}{72}$ with center (-(1/4-x/2),1/4) and another with side length $y = \frac{6-\sqrt{3}}{48}$ centered at (1/4-y/2,3/8). The tile is symmetric with respect to the angular bisector b of G_p , and so the reflections of the described squares with respect to b are also inner objects. Note that there are two outer objects, one of which, O, has a concave corner q with exterior angle $2\pi/3$. We place a parallelogram with side length x, a corner at q, and two edges contained in the edges of O incident at q. It is easy to verify that the common boundary of the inner and outer regions has a total length of 2; the inner objects are chosen such that their total perimeter is also 2.

The branch tile. If p is a branch vertex, we use the branch tile. There are two cases: G_p either contains the vertical segment from p to (0,1/2) or that from p to (0,-1/2). We specify the tile in the first case—the other can be obtained by a rotation of π . There are axis-parallel squares of side length $y = \frac{6-\sqrt{3}}{48}$ centered at $(\pm(1/4-y/2),3/8)$ and their rotations around p by angles $2\pi/3$ and $4\pi/3$. The common boundary of the inner and outer regions has a total length of $\frac{6-\sqrt{3}}{2}$, and the total perimeter of the inner objects is also $\frac{6-\sqrt{3}}{2}$.

The clause tile. If p is a clause vertex, we use the clause tile (defined in Figure 7). The other clause tiles are given by rotations of the described tile by angles $k\pi/3$ for $k=1,\ldots,5$.

4.3 Solving the tiles

Let an instance I of GEOMETRIC 3-SAT be given together with an associated fence \mathcal{F} . Consider the restriction of I to a convex polygon P and the part of the fence $\mathcal{F} \cap P$ inside P. Note that $\mathcal{F} \cap P$ consists of (not necessarily disjoint) closed curves and open curves with endpoints on the boundary ∂P , such that no two objects in P of different color can be connected by a path $\pi \subset P$ unless π intersects \mathcal{F} . (An open curve is a subset of a larger closed curve of \mathcal{F} that continues outside P.) We say that a set of closed and open curves in P with that property is a solution to $I \cap P$. In the following, we analyze the solutions to the tiles defined in Section 4.2 in order to characterize the solutions of minimum cost. We say that two closed curves (disjoint from the interiors of the objects) are homotopic if one can be continuously deformed into the other without entering the interiors of the objects. Two open curves with endpoints on the boundary of the tile are homotopic if they are subsets of two homotopic closed curves (that extends outside the tile).

Lemma 9. Figure 8 shows optimal solutions to each kind of tile. The cost in each case is:

- Straight tile: 2.
- Inner color change tile: 5/2.
- Outer color change tile: $\left(\frac{2}{\sqrt{3}} \frac{1}{2}\right) + 2 \approx 2.65$.
- Bend tile: 2.

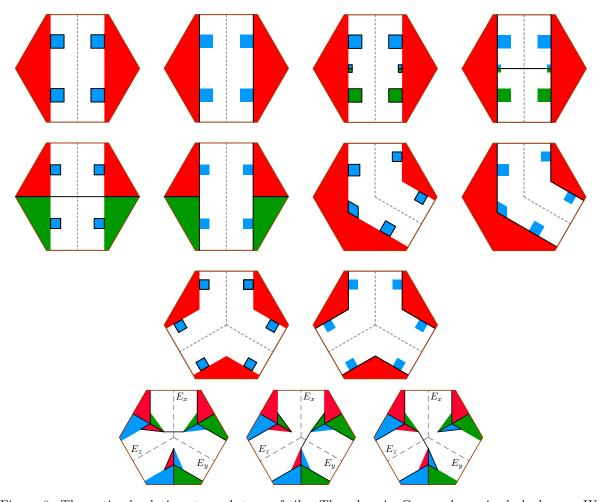


Figure 8: The optimal solutions to each type of tile. The edges in G_p are shown in dashed grey. We denote the left solution of each of the first five types of tiles as the *outer* solution and the other as the *inner* solution. For the clause tile, we define the solution as the *z-outer*, *x-outer*, and *y-outer* solution in order from left to right, respectively.

- Branch tile: $\frac{6-\sqrt{3}}{2} \approx 2.13$.
- Clause tile: $\approx 3.51.^{1}$

If the cost of a solution \mathcal{F} to a tile T exceeds the optimum by less than 1/50, then \mathcal{F} is homotopic to one of the optimal solutions \mathcal{F}^* of T in the following sense: For each curve π^* in \mathcal{F}^* , there is a curve π in \mathcal{F} homotopic to π^* . If π is closed, the distance from any point on π to the closest point on π^* is less than $\sqrt{(1/8+1/100)^2-(1/8)^2}<0.06$. If π is open and π^* has an endpoint f^* , there is a corresponding endpoint f^* of π with $||f^*f||<1/10$.

Proof. We assume that the center of the tile T is p := (0,0) and in each case, that T is rotated as in the description of the tiles and have colors as in Figure 7. We also define G_p to be the two or three half-edges of $G(\Phi)$ meeting at p as in the description of the tiles.

Consider first the case that T is any of the tiles except the clause tile. Note that G_p separates T into two or three pieces. The pieces are two pentagons for the straight, inner color change, and outer color change tiles; a pentagon and a heptagon for the bend tile; and three pentagons for the branch tile. We consider each such piece T' individually and check the minimum cost of a solution to T'. It is easy to verify that for each such piece T', there are two solutions, and they are exactly as shown in Figure 8. One solution corresponds to the outer state and the other to the inner state, and in order to be combined to a solution for all of T, each of the two or three pieces T' needs to be in the same state. It therefore follows that the solutions shown in Figure 8 are all the optimal solutions.

One can also easily verify that any solution \mathcal{F} that is not homotopic to an optimal solution has a cost that exceeds the optimal cost by more than 1/50. Suppose that the cost of a solution \mathcal{F} exceeds the cost of a homotopic optimal solution \mathcal{F}^* by less than 1/50. In order to decide how much \mathcal{F} can deviate from \mathcal{F}^* , consider the straight tile as an example, see Figure 9. In the outer state, each curve enclosing an inner object has length at least 1/2. Since the total cost is less than 2+1/50, each curve has length less than 1/2+1/50. An elementary analysis gives that a closed curve of length at most 1/2+1/50 which encloses a square of side length 1/8 is within distance $\sqrt{(1/16+1/100)^2-(1/16)^2}<0.04$ from the boundary of the square. For the inner state, consider the curve $\pi \subset \mathcal{F}$ in the right side of the tile that has the inner objects to the left. The length of π has to be less than 1+1/50 in order for the total cost to be less than 2+1/50. Note that π has to pass through the upper right corner (1/4,5/16) of the upper right square. Therefore, π has to meet the top edge of T at a point within distance $\sqrt{(3/16+1/50)^2-(3/16)^2}<0.09$ from the corresponding endpoint (1/4,1/2) of π^* . The other non-clause tiles are analyzed in a similar way.

The analysis of the clause tile is not as simple, since one does not get a solution to the complete tile by combining optimal solutions of smaller pieces. The proof has been deferred to Lemma 10 and relies on an extensive case analysis.

The largest possible deviation between a closed curve in \mathcal{F} and \mathcal{F}^* can appear for the clause tile, since it contains an inner object with the longest edge of all tiles, namely a triangle with an edge of length 1/4. That leads to a deviation of less than $\sqrt{(1/8+1/100)^2-(1/8)^2}<0.06$. Likewise, the largest possible deviation between open curves is 1/10, as realized in the clause tile and described in Lemma 10.

We now analyze the optimal solutions of the clause tile. Here, we define a *domain* as a connected component of a territory. The names of objects in the clause tile referred to in the following lemma are defined in Figure 10. Indices are taken modulo 3. The optimal solutions are covered by case 2.3.2 in the proof.

Lemma 10. The cost of a solution \mathcal{F} to a clause tile is at least $M := 3\|d_0c_0\| + 6\|e_0b_0\| + 4\|a_0b_0\| + 2\|b_0c_0\| + \|c_0c_1\|$. Moreover, if the cost is less than M + 1/50, then there is $i \in \{0, 1, 2\}$ such that \mathcal{F} contains

- a curve from $f_i \in a_i a_i'$ to b_i , where $||f_i a_i|| < \sqrt{(6/25 + 1/50)^2 (6/25)^2} = 1/10$,
- a curve from $f'_i \in a_i a'_i$ to b'_i , where $||f'_i a'_i|| < 1/10$,
- a curve from $f_{i+1} \in a_{i+1}a'_{i+1}$ to b_{i+1} , where $||f_{i+1}a_{i+1}|| < 1/10$,
- a curve from $f'_{i+1} \in a_{i+1}a'_{i+1}$ to b'_{i+1} , where $||f'_{i+1}a'_{i+1}|| < 1/10$,

¹The exact value is complicated due to the coordinates and of no use.

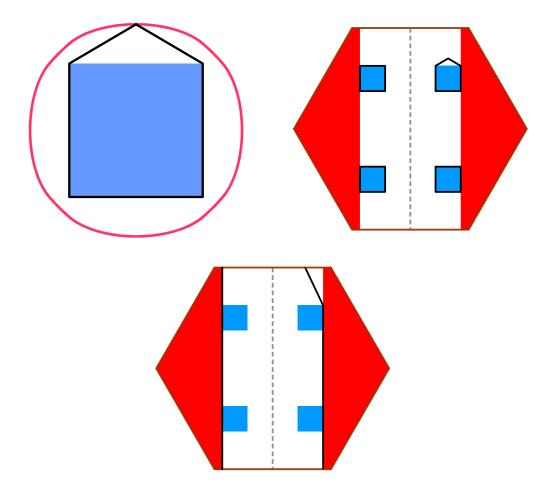


Figure 9: Left: A square of side length 1/8. The red curve encloses all curves of length at most 1/2+1/50 that enclose the square. Such a curve with maximum deviation from the boundary of the square is drawn in black. The red curve consists of a piece of each of eight different ellipses. Middle resp. right: A solution to the straight tile in the outer resp. inner state with a cost that exceeds the optimum by 1/50.

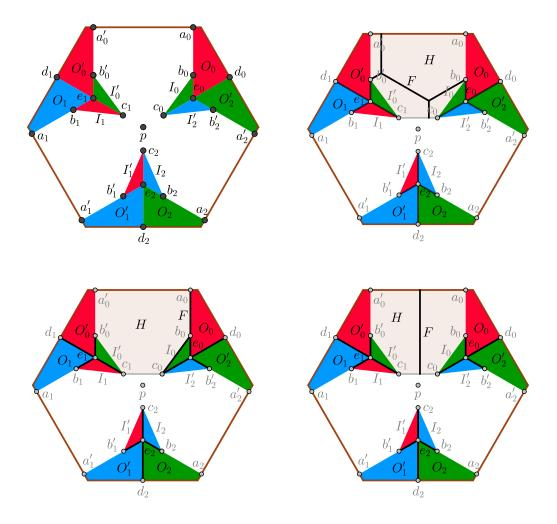


Figure 10: Top: Annotations. Case 1.1. Bottom: Case 1.2. Case 1.3.

- a curve from c_{i+1} to c_{i+2} ,
- a curve from c_i to b'_{i+2} ,
- a curve from c_{i+2} to b_{i+2} .

Proof. Clearly, \mathcal{F} must contain segments $d_i c_i$, $e_i b_i$, and $e_i b'_{i+2}$ for any $i \in \{0,1,2\}$ since each of these segments are on the shared boundary of two objects of different color. In total, this amounts for the cost $3\|d_0 c_0\| + 6\|e_0 b_0\|$. In the following, we argue about the fence needed in addition to that, i.e., the part of \mathcal{F} contained in the closed pentadecagon $T' = a_0 a'_0 b'_0 c_1 b_1 a_1 a'_1 b'_1 c_2 b_2 a_2 a'_2 b'_2 c_0 b_0$. We characterize how the solution looks when the additional cost in T' is at most $4\|a_0 b_0\| + 2\|b_0 c_0\| + \|c_0 c_1\| + 0.02 < 1.67$. When we say that the solution must contain a curve or a tree with certain properties (such as connecting two specific points), we mean such a curve or tree contained in T'.

We divide into cases after which objects are in the same domains. After making enough assumptions in one branch of the case analysis, we can either give a lower bound of the cheapest solution above 1.67, or it follows that all objects of different colors are separated, and then we state what the optimal solution satisfying the specific assumptions is. We have used Geogebra [11] to construct the solutions and estimate their costs. Each estimate differs from the exact value by at most 0.005.

Note first that for any $i \in \{0, 1, 2\}$, in order to separate O_i from I_i , the solution must contain a curve (in T') starting at b_i that has a length of at least 0.24, and similarly one from b'_i in order to separate O'_i from I'_i . The prefixes of length 0.24 of these six fences are disjoint. We therefore charge 0.24 to each b_i and b'_i .

Case 1: For a value of i, neither O_i and O'_i nor I_i and I'_i are in a domain together. Without loss of generality, suppose that the condition holds for i = 0. We consider the solution \mathcal{F} restricted to the hexagon $H = a_0 a'_0 b'_0 c_1 c_0 b_0$. In order to separate O_0 and O'_0 in H, there must be a connected component F of $\mathcal{F} \cap H$ that connects $a_0 a'_0$ and $c_0 c_1$. The individual cases are shown in Figure 10.

Case 1.1: F also separates O_0 from I_0 and O'_0 from I'_0 . Note that F connects b_0 and b'_0 . The shortest connected system of curves that connects b_0 , b'_0 , $a_0a'_0$ and c_0c_1 is a Steiner minimal tree with vertical edges meeting $a_0a'_0$ and c_0c_1 . All such trees have the same cost, which is ≈ 0.87 . But adding the 0.24 charged to b_1 , b'_1 , b_2 , b'_2 , we get more than 1.67.

Case 1.2: F separates O_0 from I_0 , but not O'_0 from I'_0 . (The case where F separates O'_0 from I'_0 , but not O_0 from I_0 , is analogous.) Note that F has minimal length if $F = a_i b_i \cup b_i c_i$, which has length ≈ 0.49 . In addition to that comes 1.2 charged to b'_i, b_{i+1}, \ldots , and the total is 1.69 > 1.67.

Case 1.3: F separates neither O_0 from I_0 , nor O'_0 from I'_0 . In this case, F has cost at least ≈ 0.44 , which is the distance between $a_i a'_i$ and $c_i c_{i+1}$. In addition comes 1.44 charged to b_i, b'_i, \ldots , which in total is more than 1.67.

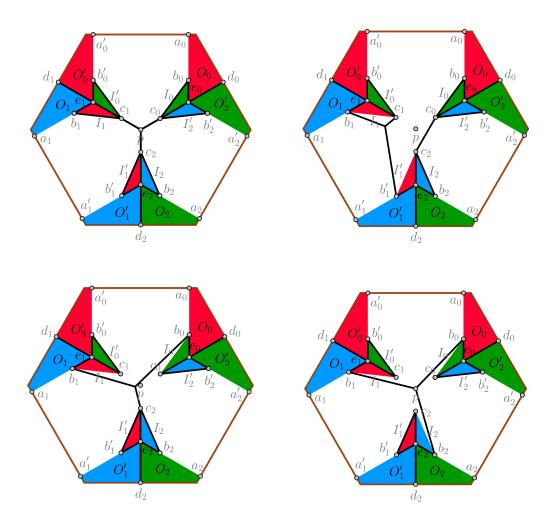


Figure 11: Top: Case 2.1.1. Case 2.1.2. Bottom: Case 2.1.3.1. Case 2.1.3.3.

Case 2: For any value of i, O_i and O'_i or I_i and I'_i are in a domain together. We may now divide into cases after how many values of i satisfy that I_i and I'_i are in the same domain. Let c denote this number.

Case 2.1: c = 0. In this case, O_i and O'_i are in the same domain for each i. The individual cases are shown in Figure 11.

Case 2.1.1: For no value of i is $O_i \cup O_i'$ in a domain with I_{i+1} or I_{i+1}' . In this case, the solution contains curves from b_i to c_i and b_i' to c_{i+1} for each i, since the objects I_i and I_i' are separated from other objects of the same color. Furthermore, there must be a curve from b_i to b_i' bounding the domain containing $O_i \cup O_i'$. It follows that the solution connects any two of the nine points $\bigcup_{i=0}^2 \{b_i, b_i', c_i\}$. The cheapest solution that satisfies this is $\bigcup_{i=0}^2 b_i c_i \cup b_i' c_{i+1} \cup c_i p$, which has $\cot \approx 1.85 > 1.67$.

Case 2.1.2: $O_i \cup O_i'$ is in a domain with I_{i+1}' . Assume without loss of generality that $O_0 \cup O_0'$ is in a domain with I_1' . The mentioned domain separates $O_1 \cup O_1'$ from I_2 and I_2' , and it separates $O_2 \cup O_2'$ from I_0' . The boundary of that domain contains a curve connecting b_0' and b_1' and one connecting b_0 and c_2 . It follows that the solution contains

- a tree connecting b'_0, c_1, b_1, b'_1 (b_1 and c_1 are connected since I_1 is isolated from the other red objects),
- a tree connecting b_0, c_2, b_2 (b_2 and c_2 are connected since I_2 is separated from the other blue objects),
- a curve connecting b'_2 and c_0 (same reasons as above).

The optimal solution of this form consists of segments from b_1, b'_1, c_1 to their Fermat point and the segments $b_0c_0, b'_0c_1, b'_2c_0, c_0c_2, b_2c_2$, and it has $\cos t \approx 1.85 > 1.67$.

Case 2.1.3: $O_i \cup O_i'$ is in a domain with I_{i+1} . Assume without loss of generality that $O_0 \cup O_0'$ is in a domain with I_1 . That domain separates $O_2 \cup O_2'$ from I_0' , and thus any solution contains a curve from b_0' to c_1 . There must also be a curve connecting b_0 and b_1 on the boundary of the domain. The solution also contains a curve from b_1' to c_2 , as I_1' is isolated from the other red objects.

Case 2.1.3.1: $O_1 \cup O'_1$ is not in a domain with I_2 or I'_2 . Any solution contains a curve from b_1 to b'_1 (bounding the domain of $O_1 \cup O'_1$), one from b_2 to c_2 (bounding the domain of I_2), and one from b'_2 to c_0 (bounding the domain of I'_2). To summarize, the solution contains

- a tree connecting b_0, b_1, b'_1, b_2, c_2 ,
- a curve connecting b'_0 and c_1 , and
- a curve connecting b'_2 and c_0 .

The shortest such solution consists of segments from b_0, b_1, c_2 to their Fermat point and the segments $b'_0c_1, b'_1c_2, b_2c_2, b'_2c_0$, and it has cost $\approx 1.83 > 1.67$.

Case 2.1.3.2: $O_1 \cup O'_1$ is in a domain with I'_2 . This case is covered by case 2.1.2.

Case 2.1.3.3: $O_1 \cup O_1'$ is in a domain with I_2 . There is a curve bounding that domain connecting b_1 and b_2 . There are thus curves connecting all pairs b_i, b_{i+1} and b_i', c_{i+1} . The shortest solution of that form is $\bigcup_{i=0}^2 b_i p \cup b_i' c_{i+1}$, which has total cost $\approx 1.83 > 1.67$.

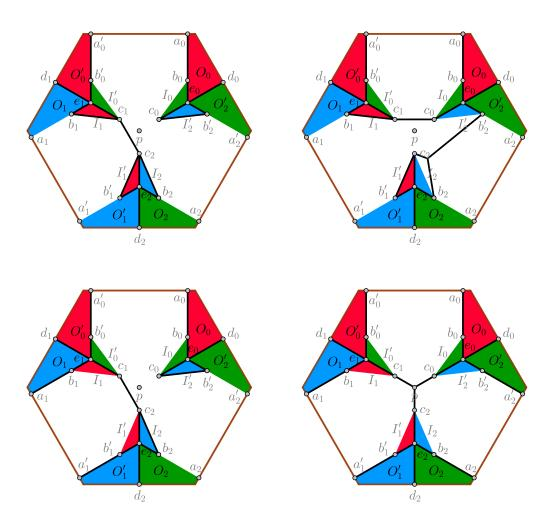


Figure 12: Top: Case 2.2.1. Case 2.2.2. Bottom: Case 2.3. Case 2.4.

Case 2.2: c = 1. Assume without loss of generality that I_0 and I'_0 are in the same domain. We thus also know that O_1 and O'_1 are in the same domain, as are O_2 and O'_2 . The domain of $I_0 \cup I'_0$ separates O_0 and O'_0 from I_1 and I'_1 , so I_1 and I'_1 are in separate domains, and the solution must contain a curve connecting b_1 and c_1 and one connecting b'_1 and c_2 bounding these domains.

Note that in order to separate $I_0 \cup I'_0$ from O_0 and O'_0 , the solution either contains a curve from b_0 to b'_0 or curves from b_0 and b'_0 to the boundary segment $a_0a'_0$. We consider the latter option, which is 0.02 cheaper. It will follow from the analysis that even this is too expensive to get below M + 0.02. The individual cases as shown in Figure 12.

Case 2.2.1: $O_1 \cup O_1'$ is not in a domain with I_2 or I_2' . The solution contains a curve from b_1 to b_1' bounding the domain containing $O_1 \cup O_1'$, and a curve connecting b_2 and c_2 , and one connecting b_2' and c_3 on the boundaries of the domains of I_2 and I_2' , respectively. It follows that the solution contains a tree connecting b_1, c_1, c_2, b_1', b_2 .

The cheapest such solution is $a_0b_0 \cup a_0'b_0' \cup b_1c_1 \cup c_1c_2 \cup b_1'c_2 \cup b_2c_2 \cup b_2'c_0$, which has cost M+0.02. This "second-best" solution is the reason we have chosen the threshold 0.02 in the lemma.

Case 2.2.2: $O_1 \cup O_1'$ is in a domain with I_2' . The solution contains a curve connecting b_1 and c_0 and one connecting b_1' and b_2' bounding that domain. It also contains a curve connecting b_2 and c_2 bounding the domain of I_2 , since I_2 is separated from the other blue objects. The optimal solution consists of segments from b_2, b_2', c_2 to their Fermat point and segments $a_0b_0, a_0'b_0', b_1c_1, b_1'c_2, c_0c_1$, and it has cost $\approx 1.83 > 1.67$.

Case 2.2.3: $O_1 \cup O_1'$ is in a domain with I_2 . The solution contains a curve connecting b_1 and b_2 , and one connecting b_2' and c_0 bounding the domain of I_2' . The cheapest solution is similar to that in case 2.2.1, where the domain containing $O_1 \cup O_1' \cup I_2$ has collapsed to zero width at c_2 .

Case 2.3: c = 2. Assume without loss of generality that I_0 and I'_0 are in the same domain, as are I_1 and I'_1 . Furthermore, I_2 and I'_2 are separated, but O_2 and O'_2 are together. As in case 2.2, we assume that O_0 and O'_0 are separated, as are O_1 and O'_1 . Otherwise, the cost of the solution will increase by at least 0.02, and as the analysis will show, that is too much to stay below M + 0.02.

The domain containing $I_1 \cup I_1'$ separates O_1 and O_1' from I_2 and I_2' . It follows that there is a curve in the solution that connects b_2 and c_2 , and one that connects b_2' and c_0 . Likewise, the domain containing $I_0 \cup I_0'$ separates O_0 and O_0' from I_1 and I_1' . Hence, the boundary of the domain containing $I_1 \cup I_1'$ contains a curve connecting c_1 and c_2 . The cheapest solution is obtained as $a_0b_0 \cup a_0'b_0' \cup a_1b_1 \cup a_1'b_1' \cup b_2c_2 \cup b_2'c_0' \cup c_1c_2$, as shown in Figure 12, and the cost is M. This is the optimal solution among all cases.

The segment a_0b_0 can be substituted by a curve from $f_0 \in a_0a'_0$ to b_0 , while keeping the cost below M + 0.02, if and only if $||f_0a_0|| < \sqrt{(0.24 + 0.02)^2 - 0.24^2} = 0.1$. Likewise for the other segments with an endpoint on the boundary of T. These are exactly the solutions described in the lemma.

Case 2.4: c=3. The cheapest solution is obtained when O_i and O'_i are separated for each i. Furthermore, the solution contains a curve connecting c_i and c_{i+1} for each i bounding the domain containing $I_i \cup I'_i$. The cheapest such solution is $\bigcup_{i=0}^2 a_i b_i \cup a'_i b'_i \cup c_i p$ as shown in Figure 12, which has cost 1.79 > 1.67.

Theorem 11. The problem GEOMETRIC 3-CUT is NP-hard.

Proof. Let an instance $(\Phi, G(\Phi))$ of COLORED TRIGRID POSITIVE 1-IN-3-SAT be given and construct the tiles on top of $G(\Phi)$ as described. Let \mathcal{T} be the set of tiles and \mathcal{A} the area that the tiles cover (i.e., \mathcal{A} is a union of the hexagons). We will cover any holes in \mathcal{A} with completely red tiles, and place red tiles all the way along the exterior boundary of \mathcal{A} . Let \mathcal{R} be the set of these added red tiles and let I be the resulting instance of GEOMETRIC 3-CUT. It is now trivial how to place the fences in I everywhere except in the interior of \mathcal{A} .

Consider a fence \mathcal{F} to the obtained instance with cost M. Let M^* be the sum of the cost of an optimal solution to each tile in \mathcal{T} plus the cost of the fence that must be placed along the boundaries of the added red tiles in \mathcal{R} . We claim that if Φ is satisfiable, then a solution realizing the minimum M^* exists. Furthermore, if $M < M^* + 1/50$, then Φ is satisfiable.

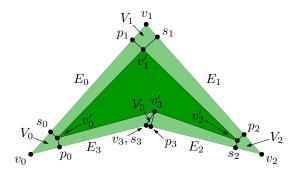


Figure 13: An object O and the rationalized version $O' \subset O$.

Suppose that Φ is satisfiable and fix a satisfying assignment. Consider a clause tile where E_x , E_y , and E_z meet. Now, we choose the v-outer state, where $v \in \{x, y, z\}$ is the variable that is satisfied. For each non-clause tile that covers a part of E_w for a variable w of Φ , we choose the outer state if w is true and the inner otherwise. It is now easy to see that the curves form a fence of the desired cost.

On the other hand, suppose that $M < M^* + 1/50$. It follows that in each tile in \mathcal{T} , the cost exceeds the optimum by at most 1/50. Hence, the solution in each tile is homotopic to one of the optimal states as described in Lemma 9. We now claim that the states of all tiles representing one variable must agree on either the inner or outer state. Consider two adjacent tiles where one is in the inner state. There are open curves with endpoints on the shared edge of the two tiles with a distance of more than $1/2 - 2 \cdot 1/10 = 3/10$. The other tile cannot be in the outer state, because then there would have to be an extra open curve of length at least 3/10 to connect those endpoints. It follows that the other tile must also be in the inner state. Thus, both tiles are either in the inner or in the outer state, as desired.

We now describe how to obtain a satisfying assignment of Φ . Consider a clause tile where E_x , E_y , and E_z meet and suppose the tile is in the x-outer state. It follows from the above that each tile covering E_x is in the outer state or, in the case of the clause tile, in the x-outer state. Similarly, each non-clause tile covering only E_y (resp. E_z) is in the inner state and each clause tile covering a part of E_y (resp. E_z) is not in the y-outer (resp. z-outer) state. We now set x to true and y and z to false and do similarly with the other clause tiles, and it follows that we get a solution to Φ .

For each object O with corner v with an irrational coordinate, we choose a substitute $v' \in O$ with rational coordinates such that $||vv'|| < \frac{1/50}{4n}$ and such that v' only requires polynomially many bits to represent. This results in an instance I' where all objects are subsets of corresponding objects in I. Let C and C' be the cost of the optimal solutions to I and I', respectively, and note that $C' \leq C$, as any solution to I is also a solution to I'. We claim that C < C' + 1/50. To prove this, consider a solution $\mathcal F$ to I'. If $\mathcal F$ contains a curve π' in the interior of an object O of I, we move π' to a curve π on the boundary of O, as follows.

Let $O' \subseteq O$ be the object in I' corresponding to O. Let v_0, \ldots, v_{k-1} be the vertices of O in clockwise order and v'_0, \ldots, v'_{k-1} the corresponding vertices of O'. In the following, indices will be taken modulo k. We divide the annulus $\mathcal{D} := \operatorname{int} O \setminus \operatorname{int} O'$ into a region E_i for each edge $v'_i v'_{i+1}$ and a region V_i for each vertex v'_i of O', see Figure 13. We make a line segment from v'_i to the closest point p_i on $v_{i-1}v_i$ and one to the closest point s_i on $v_i v_{i+1}$. We then define quadrilaterals $V_i := v'_i s_i v_i p_i$ and $E_i := v_i v_{i+1} p_{i+1} s_{i+1}$. We now describe the modification we make on π' in order to avoid \mathcal{D} . If π' intersects V_i , we remove $\pi' \cap V_i$ and instead add the segments $p_i v_i \cup v_i s_i$. Note that these added segments have total length less than $\frac{1}{100n}$. If π' intersects E_i , we project each point in $\pi' \cap E_i$ to the closest point on $v_i v_{i+1}$. This does not increase the length of the curve. It follows that the modification of π' made to avoid \mathcal{D} increases the length by less than $\frac{k}{100n}$. Performing the same operation for all objects of I', we get a solution to I with cost less than C' + 1/100. Hence, C < C' + 1/100.

cost less than C'+1/100. Hence, C < C'+1/100.

Let $M' := \frac{\lceil 100M^* \rceil}{100}$, so that M' is rational and $M^* \le M' < M^* + 1/100$. We conclude by observing that if $C' \le M'$, then $C < C' + 1/100 < M' + 1/100 < M^* + 1/50$, and thus Φ is satisfiable. On the other hand, if Φ is satisfiable, then $C' \le C = M^* \le M'$. We can thus tell whether Φ is satisfiable or not by evaluating whether $C' \le M'$.

5 Approximation

The approach for k=2 from Section 3 does not extend to $k \geq 3$ because Lemma 3 does not apply: The arrangement \mathcal{A} (formed by the free segments between the corners N of the input objects) is no longer guaranteed to contain an optimal fence, see Figure 2. However, we can still search for an approximate solution in \mathcal{A} : We show that the optimal fence $F_{\mathcal{A}}$ contained in \mathcal{A} has a cost which is at most 4/3 times higher than the true optimal fence F^* (Section 5.1). We construct a corresponding lower-bound example with $|F_{\mathcal{A}}| > 1.15 \cdot |F^*|$. (This factor is the conjectured Steiner ratio, see Section 5.2.)

The graph-theoretic problem that we then have to solve in the weighted dual graph G = (V, E) of \mathcal{A} is the *colored multiterminal cut problem*: We have terminals of $k \geq 3$ different colors and want to make a cut that separates every pair of terminals of different colors. This problem is NP-hard, but we can use approximation algorithms, see Section 5.3.

5.1 Upper bound $|F_A|/|F^*| \le 4/3$

Theorem 12. $|F_A| \le 4/3 \cdot |F^*|$.

Proof. By Lemma 1 and Lemma 2, we know that after cutting an optimal fence F^* at all points of N, the remaining components are Steiner minimal trees with leaves in N and internal *Steiner vertices* of degree 3, where three segments make angles of $2\pi/3$.

Consider such a Steiner tree T (Figure 14a). Since T is embedded in the plane, the leaves can be enumerated in cyclic order as v_1, \ldots, v_m . We will replace T by a connected system \bar{T} of fences that connects the same set of leaves v_1, \ldots, v_m , but contains only segments from the arrangement A. Furthermore, we prove that the total length of \bar{T} is bounded as $|\bar{T}| \leq \frac{4}{3}|T|$. Thus, carrying out this replacement for every Steiner tree leads to the fence F_A of the desired cost. If T consists of a single segment, we define \bar{T} to be the same segment, in which case trivially $|\bar{T}| \leq \frac{4}{3}|T|$. Assume therefore that T has at least one Steiner vertex.

Let T_{ij} be the path in T from v_i to v_j . For each pair $\{i, j\}$, we define the path \bar{T}_{ij} as the shortest path with the properties that

- a) \bar{T}_{ij} has endpoints v_i and v_j , and
- b) \bar{T}_{ij} is homotopic to T_{ij} : this means that T_{ij} can be continuously deformed into \bar{T}_{ij} while keeping the endpoints fixed at v_i and v_j , without entering the interiors of the objects.

It is clear that

- c) \bar{T}_{ij} is contained in the arrangement \mathcal{A} , and
- d) \bar{T}_{ij} is at most as long as T_{ij} .

We will construct \bar{T} as the union of paths \bar{T}_{ij} that are specified by a certain set S of leaf pairs $\{i, j\}$, and we will show that its total length is bounded $|\bar{T}| \leq \frac{4}{3}|T|$. The fact that F_A is a valid fence is ensured by our choice of the set S, which we will now discuss.

If we overlay all paths T_{ij} for $\{i,j\} \in S$, we get a multigraph \widetilde{T} , which has the same vertices as T and uses the edges of T, some of them multiple times. We require these three properties:

- 1. Every edge of T is used once or twice in \widetilde{T} .
- 2. Every Steiner vertex of T has even degree (4 or 6) in \widetilde{T} . (By contrast, the degree in T is always 3.)
- 3. Any two paths T_{ij} and $T_{i'j'}$ that have a point of T in common must cross in the following sense: If we assume, by relabeling if necessary, that i < j and i' < j', then $i \le i' \le j \le j'$ or $i' \le i \le j' \le j$.

The last property is important to ensure that \bar{T} is connected. For this we use the following lemma, whose proof is given later. For a path P and points $x, y \in P$, we denote by P[x, y] the subpath of P from x to y. This is in general not well-defined unless P is simple. To make the notation unambiguous, we will assume that the points x, y are associated to particular parameter values along the parameterization of P.

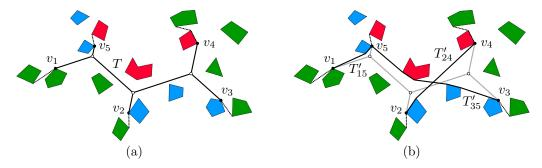


Figure 14: (a) a single Steiner tree T with 5 terminals v_1, \ldots, v_5 , part of a larger fence system F^* . Steiner vertices are white, leaves are black. (b) The transformed graph \bar{T} , formed as the union of three shortest homotopic paths \bar{T}_{15} , \bar{T}_{24} , and \bar{T}_{35} .

Lemma 13. Suppose that the paths T_{ij} and $T_{i'j'}$ cross in the sense of Property 3. Then there exists a point $\bar{x} \in \bar{T}_{ij} \cap \bar{T}_{i'j'}$ such that the path

$$\bar{T}_{ij}[v_j,\bar{x}]\cup\bar{T}_{i'j'}[\bar{x},v_{i'}]$$

is homotopic to the path $T_{ii'}$.

As we will prove shortly, Properties 1 and 3 imply that for any two leaves v_i and v_j (where the pair $\{i,j\}$ is not necessarily in S), the set \bar{T} contains a path from v_i to v_j that is homotopic to the path T_{ij} . This means that after replacing T by \bar{T} in F^* , we get a system of fences F' that encloses and separates the same objects as F^* , and thus we have indeed produced a valid fence.

We now show the existence of a path in \bar{T} homotopic to T_{ij} : Let the vertices of T_{ij} be $x_0, x_1, \ldots, x_{p+1}$ in order, such that $x_0 := v_i$ and $x_{p+1} := v_j$. For each $m = 0, 1, \ldots, p$, we select, by Property 1, a path $T_{k_m l_m}$ with $\{k_m, l_m\} \in S$ that goes through the directed edge $x_m x_{m+1}$ on the way from v_{k_m} to v_{k_l} . This leads to a sequence of paths $T_{k_0 l_0}, T_{k_1 l_1}, \ldots, T_{k_p l_p}$, where $k_0 = i$, $l_p = j$, and any two successive paths $T_{k_{m-1} l_{m-1}}$ and $T_{k_m l_m}$ have the point x_m in common, and hence cross, by Property 3. Lemma 13 implies that also the corresponding paths $\bar{T}_{k_{m-1} l_{m-1}}$ and $\bar{T}_{k_m l_m}$ have a common point \bar{x}_m such that

$$\bar{U}_m := \bar{T}_{k_{m-1}l_{m-1}}[v_{l_{m-1}}, \bar{x}_m] \cup \bar{T}_{k_m l_m}[\bar{x}_m, v_{k_m}]$$

is homotopic to $U_m := T_{l_{m-1}k_m}$. Now, define the paths

$$\begin{split} W &:= T_{k_0 l_0} \cup U_1 \cup T_{k_1 l_1} \cup U_2 \cup \ldots \cup U_p \cup T_{k_p l_p}, \text{ and } \\ \bar{W} &:= \bar{T}_{k_0 l_0} \cup \bar{U}_1 \cup \bar{T}_{k_1 l_1} \cup \bar{U}_2 \cup \ldots \cup \bar{U}_p \cup \bar{T}_{k_p l_p}. \end{split}$$

The paths T_{ij} and W are homotopic, as they have the same endpoints and W is obtained by joining paths in the simple tree T. Also, W and \bar{W} are homotopic, as the corresponding subpaths are homotopic. The paths T_{ij} and \bar{W} are thus homotopic, and \bar{W} is contained in \bar{T} , so we are done.

Proof of Lemma 13. We first describe how T_{ij} can be continuously deformed into \bar{T}_{ij} while remaining a polygonal path, moving one vertex at a time. We denote by \hat{T}_{ij} the current path during this deformation procedure.

Consider the case that \hat{T}_{ij} has a vertex b which is not in N. Let a and c be the neighboring vertices. We then move b towards c, thus shortening the edge bc while the edge ab sweeps over a region in the plane. If ab hits the corner of an object, \hat{T}_{ij} gets a new vertex a' at this point. The segment aa' will then remain static, and we continue the movement of b with a' taking the role of a. When b eventually reaches c, the number of vertices of \hat{T}_{ij} that are not in N has decreased by 1. We repeat this process of contracting edges as long as there is a vertex not in N. Note that it is possible that the path crosses itself during the deformation, or it may have a vertex where it turns 180° back on itself. Such a vertex is known as a spur, and it can be easily eliminated by moving it to the closest adjacent vertex.

(For establishing Theorem 12, we could already stop the deformation procedure as soon as all vertices of \hat{T}_{ij} are in N and \hat{T}_{ij} is free of spurs, because \hat{T}_{ij} is contained in \mathcal{A} and is at most as long as T_{ij} , thus satisfying properties (c) and (d).) If \hat{T}_{ij} is not yet the shortest homotopic path, it must contain three

consecutive vertices abc such that the angle at b contains no object. In this case we can start the same deformation move from b towards c as above. Temporarily, the vertex b is an additional vertex not in N, but after the move, \hat{T}_{ij} is again a path connecting vertices of N. Since the number of such paths that are not longer than the initial path T_{ij} is finite, the procedure must eventually terminate with the shortest homotopic path \bar{T}_{ij} .

We successively apply this procedure to the pairs ij and i'j'. We still have to prove the existence of a point $\bar{x} \in \bar{T}_{ij} \cap \bar{T}_{i'j'}$ with the property stated in the lemma. We assume that the four corners $v_i, v_j, v_{i'}, v_{j'}$ are distinct because otherwise the statement follows easily if we choose a shared endpoint as \bar{x} .

The proof uses that fact that the number of *crossings* between the paths \hat{T}_{ij} and $\hat{T}_{i'j'}$ can only change by an even number during a deformation. The definition of a crossing requires some care, as the paths may share segments. Assume that \hat{T}_{ij} is the path that is currently being deformed, while $\hat{T}_{i'j'}$ is either the initial path $T_{i'j'}$ or the final deformed path $\bar{T}_{i'j'}$.

Orient the paths \hat{T}_{ij} and $\hat{T}_{i'j'}$ arbitrarily. Consider a maximal subpath Q that is shared between \hat{T}_{ij} and $\hat{T}_{i'j'}$, possibly in opposite directions. If \hat{T}_{ij} enters and leaves Q on the same side of $\hat{T}_{i'j'}$, we say that \hat{T}_{ij} touches $\hat{T}_{i'j'}$ at Q. Otherwise, \hat{T}_{ij} and $\hat{T}_{i'j'}$ form a crossing at Q. Here it is important that $\hat{T}_{i'j'}$ has no spurs, since at a spur, the side on which \hat{T}_{ij} enters or leaves $\hat{T}_{i'j'}$ is ill-defined. If Q contains an endpoint q of one of the paths, we extend this path into the interior of the object in order to determine the side of $\hat{T}_{i'j'}$ on which \hat{T}_{ij} enters or leaves Q at q.

A crossing Q of \hat{T}_{ij} and $\hat{T}_{i'j'}$ is a homotopic crossing if it has the desired property for the lemma, namely that $\hat{T}_{ij}[v_j, \hat{x}] \cup \hat{T}_{i'j'}[\hat{x}, v_{i'}]$ for $\hat{x} \in Q$ is homotopic to $T_{ji'}$. Clearly, this does not depend on the choice of $\hat{x} \in Q$, because Q is represented by a connected interval of parameters, both on \hat{T}_{ij} and $\hat{T}_{i'j'}$.

When \hat{T}_{ij} is deformed by moving one vertex at a time, as described above, it is easy to see that crossings can only appear or disappear in pairs: It is not possible for a crossing Q to appear or disappear by \hat{T}_{ij} sliding over an endpoint q' of $\hat{T}_{i'j'}$, since that would require \hat{T}_{ij} to enter the interior of the object with q' on the boundary.

Furthermore, a pair of crossings Q_1, Q_2 that appear or disappear will either both be homotopic crossings or non-homotopic crossings: At the moment when the pair appears or disappears, the loop formed by the subpaths of \hat{T}_{ij} and $\hat{T}_{i'j'}$ between Q_1 and Q_2 is empty and thus contains no objects. Therefore, if $\hat{x}_1 \in Q_1$ and $\hat{x}_2 \in Q_2$, the paths $\hat{T}_{ij}[v_j, \hat{x}_1] \cup \hat{T}_{i'j'}[\hat{x}_1, v_{i'}]$ and $\hat{T}_{ij}[v_j, \hat{x}_2] \cup \hat{T}_{i'j'}[\hat{x}_2, v_{i'}]$ are homotopic.

During the deformation of \hat{T}_{ij} , each crossing Q can move back and forth on $\hat{T}_{i'j'}$, expand and shrink. However, it is clear that its character (homotopic versus non-homotopic) does not change during the deformation.

The initial number of crossings is 1, and the crossing, Q, is a homotopic crossing, since $T_{ji'}$ can be realized as a path $\hat{T}_{ij}[v_j, \hat{x}] \cup \hat{T}_{i'j'}[\hat{x}, v_{i'}]$ for $\hat{x} \in Q$. Hence the number of homotopic crossings of \bar{T}_{ij} and $\bar{T}_{i'j'}$ is odd, and in particular positive, which establishes the claim.

To bound the length of \bar{T} , we bound each path \bar{T}_{ij} , $\{i,j\} \in S$, by the corresponding path T_{ij} in T. This upper estimate is simply the total length of T plus the length of the duplicated edges of T.

Our first task is to construct the multigraph \widetilde{T} . By Property 1, this boils down to selecting which edges of T to duplicate. In order to fulfill Property 2, we require that the degree of every inner vertex of \widetilde{T} becomes even. (We show later that this is sufficient to ensure that the edges of \widetilde{T} can be partitioned into paths T_{ij} subject to Property 3.)

Lemma 14. The edges that should be duplicated can be chosen such that their total length is at most |T|/3.

Proof. For a particular tree, the optimum can be computed easily by dynamic programming, as follows. We root T at some arbitrary leaf. Consider a subtree U rooted at some vertex u of T such that u has one child v in U. We define U_1 and U_2 as the cost of the optimal set of duplicated edges in U, under the constraint that the multiplicity of the edge uv in \widetilde{T} is 1 and 2, respectively.

By induction, we will establish that

$$2U_1 + U_2 \le |U|. (1)$$

This gives $\min\{U_1, U_2\} \leq |U|/3$ and proves the lemma, since this also holds for U = T.

In the base case U has only one edge. Then $U_1 = 0$ and $U_2 = ||uv|| = |U|$, and (1) holds.

If U is larger, v has degree 3, and two subtrees L and R are attached there. If uv is not duplicated, then exactly one of the other edges incident to v has to be duplicated in order for v to get even degree in \widetilde{T} . On the other hand, if uv is duplicated, then either both or none of the other edges should be duplicated. Hence, we can compute U_1 and U_2 by the following recursion:

$$U_1 = \min\{L_1 + R_2, L_2 + R_1\} \tag{2}$$

$$U_2 = \min\{L_1 + R_1, L_2 + R_2\} + \|uv\| \tag{3}$$

We therefore get

$$U_1 \le L_2 + R_1 \tag{4}$$

$$U_1 \le L_1 + R_2 \tag{5}$$

from (2) and

$$U_2 \le L_1 + R_1 + \|uv\| \tag{6}$$

from (3). Adding inequalities (4–6) and using the inductive hypothesis (1) for L and R gives

$$2U_1 + U_2 \le 2L_1 + L_2 + 2R_1 + R_2 + ||uv|| \le |L| + |R| + ||uv|| = |U|.$$

The bound |T|/3 in Lemma 14 cannot be improved, as shown by the graph $K_{1,3}$ with unit edge lengths. This graph can appear as a Steiner tree in an optimal fence, see Figure 15. (But this does not mean that the factor 4/3 in Theorem 12 cannot be improved.)

We now have a multigraph \widetilde{T} where every internal vertex has even degree. It follows that the edges of \widetilde{T} can be partitioned into leaf-to-leaf paths, much like when creating an Eulerian tour in a graph where all vertices have even degree.

We still need to satisfy Property 3. Whenever two paths P_1 and P_2 violate this property, we repair this by swapping parts of the paths, without changing the number of remaining violating pairs, as follows: The paths P_1 and P_2 must have a common vertex, and thus also a common edge uv, because the maximum degree in T is 3. Orient P_1 and P_2 so that they use this edge in the direction uv, and cut them at v into $P_1 = Q_1 \cdot R_1$ and $P_2 = Q_2 \cdot R_2$. We now make a cross-over at v, forming the new paths $Q_1 \cdot R_2$ and $Q_2 \cdot R_1$. These new paths satisfy Property 3. To check that we did not create any new violations, we observe that, by Property 1, no other path can use the edge uv, because the capacity of 2 is already taken by P_1 and P_2 . Thus, all other paths can either interact with Q_1 and Q_2 , or with R_1 and R_2 . Thus, swapping the parts of P_1 and P_2 in the other half of the tree T does not affect Property 3.

We have thus established Theorem 12. \Box

5.2 Lower bound on $|F_A|/|F^*|$

We believe that the bound of Theorem 12 can be improved: We bounded $|\bar{T}_{ij}|$ crudely by $|T_{ij}|$, using only the triangle inequality, and we did not use at all the fact that edges meet at 120°.

We construct an example that establishes a lower bound. Gilbert and Pollack [9] conjectured that for any set of points in the plane, the ratio between the length of a minimum spanning tree and the length of a minimum Steiner tree is at most $\frac{2}{\sqrt{3}} \approx 1.15$, which is realized by the corners of an equilateral triangle. The current best upper bound is 1.21 by Chung and Graham [6]. We show a lower bound on the ratio $|F_A|/|F^*|$ that corresponds to the conjectured Steiner ratio.

Lemma 15. For every $\varepsilon > 0$, there is an instance of GEOMETRIC 3-CUT for which

$$\frac{|F_{\mathcal{A}}|}{|F^{\star}|} \ge \frac{2}{\sqrt{3}} - \varepsilon > 1.15 - \varepsilon.$$

Proof. The core idea is shown in Figure 15: Three very thin rectangles in different colors form an equilateral triangle with side length $\sqrt{3}$. The optimal fence uses the center of the triangle as a Steiner vertex, whereas the fence $F_{\mathcal{A}}$ is restricted to follow the triangle edges. This example, considered in isolation, gives only a ratio $|F_{\mathcal{A}}|/|F^*| \approx (4\sqrt{3})/(3+2\sqrt{3}) \approx 1.07$, because the outer boundary edges, which are common to both fences, "dilute" the ratio.

So we set $k=1/\varepsilon$, and repeat the construction $k\times k$ times. We get $|F^{\star}|=2k^2\cdot 3+2k\cdot \sqrt{3}$, versus $|F_{\mathcal{A}}|=2k^2\cdot 2\sqrt{3}+2k\cdot \sqrt{3}$.

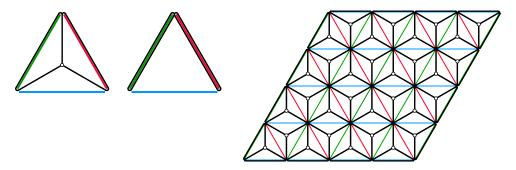


Figure 15: The core (left) and repeated (right) construction from the proof of Lemma 15.

5.3 Finding a good fence in A

The problem of finding a small cut in a planar graph G = (V, E) that separates k different classes $T_1, \ldots, T_k \subset V$ of terminals was mentioned as a suggestion for future work by Dahlhaus et al. [7], but we have not found any subsequent work on that except for the case k = 2 [3]. We can, however, reduce the problem to the multiway cut problem in general graphs (also known as the multiterminal cut problem): For each class T_i , we add an "apex vertex" t_i which is connected to all vertices in T_i by edges of infinite weight. We then ask for the cut of minimum total weight that separates each pair t_i, t_j . Dahlhaus et al. gave a (2 - 2/k)-approximation algorithm for the problem. In our setup, the running time will be $O(kn^8 \log n)$. The approximation ratio was since then improved to 3/2 - 1/k by Călinescu et al. [4]. Finally, a randomized algorithm with approximation factor 1.3438 was given by Karger et al. [12], who also gave the best known bounds for various specific values of k. Together with Theorem 12, we obtain the following result.

Theorem 16. There is a randomized $4/3 \cdot 1.3438$ -approximation algorithm and a deterministic $(2 - \frac{4}{3k})$ -approximation algorithm for GEOMETRIC k-CUT, each of which runs in polynomial time.

Acknowledgements

This work was initiated at the workshop on *Fixed-Parameter Computational Geometry* at the Lorentz Center in Leiden in May 2018. We thank the organizers and the Lorentz Center for a nice workshop and Michael Hoffmann for useful discussions during the workshop.

References

- [1] Mikkel Abrahamsen, Anna Adamaszek, Karl Bringmann, Vincent Cohen-Addad, Mehran Mehr, Eva Rotenberg, Alan Roytman, and Mikkel Thorup. Fast fencing. In *Proceedings of the 50th Annual ACM SIGACT Symposium on Theory of Computing*, STOC 2018, pages 564–573, 2018.
- [2] Oswin Aichholzer and Franz Aurenhammer. Straight skeletons for general polygonal figures in the plane. In *Computing and Combinatorics (COCOON 1996)*, pages 117–126, 1996.
- [3] Glencora Borradaile, Philip N. Klein, Shay Mozes, Yahav Nussbaum, and Christian Wulff-Nilsen. Multiple-source multiple-sink maximum flow in directed planar graphs in near-linear time. SIAM Journal on Computing, 46(4):1280–1303, 2017.
- [4] Gruia Călinescu, Howard Karloff, and Yuval Rabani. An improved approximation algorithm for multiway cut. *Journal of Computer and System Sciences*, 60(3):564–574, 2000.
- [5] Bernard Chazelle and Herbert Edelsbrunner. An optimal algorithm for intersecting line segments in the plane. J. ACM, 39(1):1–54, 1992.
- [6] Fan R. K. Chung and Ronald L. Graham. A new bound for Euclidean Steiner minimum trees. Ann. N.Y. Acad. Sci., 440:328–346, 1986.

- [7] Elias Dahlhaus, David S. Johnson, Christos H. Papadimitriou, Paul D. Seymour, and Mihalis Yannakakis. The complexity of multiterminal cuts. SIAM Journal on Computing, 23(4):864–894, 1994.
- [8] Paweł Gawrychowski and Adam Karczmarz. Improved bounds for shortest paths in dense distance graphs, 2016. https://arxiv.org/abs/1602.07013.
- [9] Edgar N. Gilbert and Henry O. Pollak. Steiner minimal trees. SIAM Journal on Applied Mathematics, 16(1):1–29, 1968.
- [10] Dorothy M. Greig, Bruce T. Porteous, and Allan H. Seheult. Exact maximum a posteriori estimation for binary images. *Journal of the Royal Statistical Society. Series B (Methodological)*, 51(2):271–279, 1989.
- [11] Markus Hohenwarter, Michael Borcherds, Gabor Ancsin, Balázs Bencze, Mathieu Blossier, Arnaud Delobelle, Calixte Denizet, Judit Éliás, Arpad Fekete, Laszlo Gál, Zbynek Konečný, Zoltan Kovács, Stefan Lizelfelner, Bernard Parisse, and George Sturr. GeoGebra 5.0, 2018. http://www.geogebra.org.
- [12] David R. Karger, Philip Klein, Cliff Stein, Mikkel Thorup, and Neal E. Young. Rounding algorithms for a geometric embedding of minimum multiway cut. *Mathematics of Operations Research*, 29(3):436–461, 2004.
- [13] Wolfgang Mulzer and Günter Rote. Minimum-weight triangulation is NP-hard. *Journal of the ACM*, 55:Article 11, 29 pp., May 2008.